LETTERS

High-resolution multi-dimensional NMR spectroscopy of proteins in human cells

Kohsuke Inomata[1,2], Ayako Ohno[1], Hidehito Tochio[1,2], Shin Isogai[1], Takeshi Tenno[2,4], Ikuhiko Nakase[5], Toshihide Takeuchi[5], Shiroh Futaki[3,5], Yutaka Ito[2,6], Hidekazu Hiroaki[2,4] & Masahiro Shirakawa[1,2,7]

In-cell NMR is an isotope-aided multi-dimensional NMR technique that enables observations of conformations and functions of proteins in living cells at the atomic level[1]. This method has been successfully applied to proteins overexpressed in bacteria, providing information on protein–ligand interactions[2] and conformations[3,4]. However, the application of in-cell NMR to eukaryotic cells has been limited to *Xenopus laevis* oocytes[5–7]. Wider application of the technique is hampered by inefficient delivery of isotope-labelled proteins into eukaryote somatic cells. Here we describe a method to obtain high-resolution two-dimensional (2D) heteronuclear NMR spectra of proteins inside living human cells. Proteins were delivered to the cytosol by the pyrenebutyrate-mediated action of cell-penetrating peptides[8] linked covalently to the proteins. The proteins were subsequently released from cell-penetrating peptides by endogenous enzymatic activity or by autonomous reductive cleavage. The heteronuclear 2D spectra of three different proteins inside human cells demonstrate the broad application of this technique to studying interactions and protein processing. The in-cell NMR spectra of FKBP12 (also known as FKBP1A) show the formation of specific complexes between the protein and extracellularly administered immunosuppressants, demonstrating the utility of this technique in drug screening programs. Moreover, in-cell NMR spectroscopy demonstrates that ubiquitin has much higher hydrogen exchange rates in the intracellular environment, possibly due to multiple interactions with endogenous proteins.

We have established a method to observe in-cell NMR spectra of ^{15}N-labelled proteins, which are delivered to cells by cell-penetrating peptides (CPPs)[9–11]. First, the CPP sequence of Tat from HIV-1 (ref. 12) (CPP_{Tat}: 47-YGRKKRRQRRR-57) was fused to the carboxy terminus of a human ubiquitin derivative containing alanine substitutions at Leu 8, Ile 44 and Val 70 (designated Ub-3A). The fusion protein Ub-3A–CPP_{Tat} (Fig. 1a) was uniformly labelled with ^{15}N, and then incubated with human HeLa cells in the presence of pyrenebutyrate (1-pyrenebutyric acid), which mediates the direct translocation of CPP-linked proteins into the cytosol[8]. The 2D ^{1}H–^{15}N correlation spectrum of the cells gave well-resolved cross-peaks, showing a pattern typical of a stably folded and homogeneously dispersed protein (Fig. 1a). Comparison with the reference *in vitro* spectrum (Fig. 1b) showed that the positions of most cross-peaks were well preserved in the in-cell spectrum. However, an intense signal was observed at a position corresponding to the C-terminal Gly 76 of mature ubiquitin in the in-cell spectrum, but not in the *in vitro* spectrum. Conversely, the cross-peak of the C-terminal residue of CPP_{Tat} was missing in the in-cell spectrum. This observation suggested that the Ub-3A–CPP_{Tat} fusion protein was cleaved between Gly 76 and Asp 77—presumably by a group of endogenous ubiquitin-specific C-terminal proteases (DUBs)[13]—and that the clipped CPP peptide was not observed in the in-cell NMR spectrum (Fig. 1a and Supplementary Fig. 1). Cleavage of Ub-3A–CPP_{Tat} in the cells was further confirmed by electrophoretic analysis of transduced fluorescently labelled protein (Supplementary Fig. 1c). Because DUBs are localized in the cytosolic

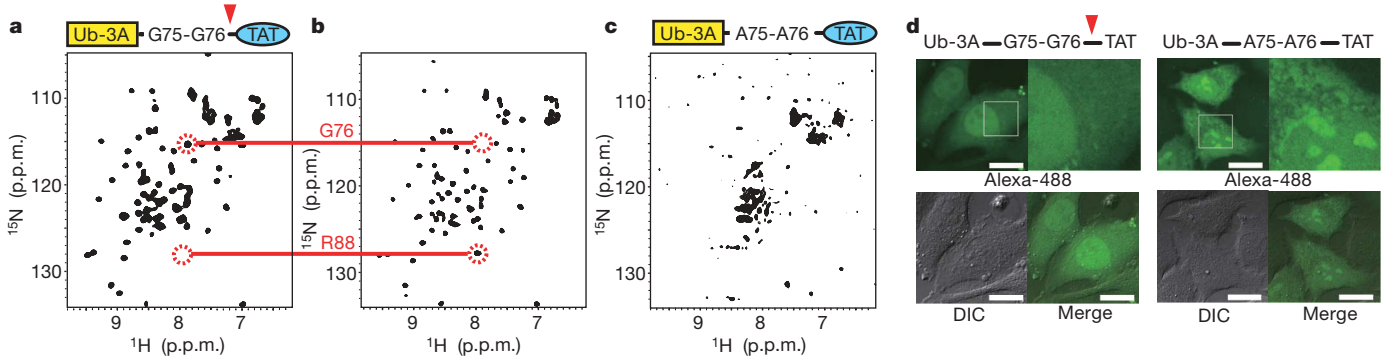

Figure 1 | In-cell NMR spectra and cellular distribution of transduced ubiquitin derivative. a, Spectrum of Ub-3A in HeLa cells. The cross-peak of the C-terminal Gly 76 is indicated. **b**, *In vitro* reference spectrum of the ^{15}N Ub-3A–CPP_{Tat} fusion. The cross-peak of arginine at the C-terminal end of CPP_{Tat} (Arg 88) is indicated. **c**, Spectrum of HeLa cells treated with ^{15}N Ub-3A-G75A/G76A–CPP_{Tat}. **d**, Distribution of transduced Alexa-488-labelled Ub-3A–CPP_{Tat} and Ub-3A-G75A/G76A–CPP_{Tat} in HeLa cells observed by confocal laser-scanning microscopy. DIC, differential interference contrast. Scale bars, 20 μm. In **a** and **c**, the constructs used for intracellular transduction are schematically shown above the spectrum. The DUB cleavage site is indicated by a red triangle.

[1]Department of Molecular Engineering, Graduate School of Engineering, Kyoto University, Nishikyo-Ku, Kyoto 615-8510, Japan. [2]CREST, and [3]SORST, JST, 4-1-8 Honcho, Kawaguchi, Saitama 332-0012, Japan. [4]Division of Structural Biology, Graduate School of Medicine, Kobe University, 7-5-1, Kusunoki-cho Chuo-ku, Kobe, Hyogo 650-0017, Japan. [5]Institute for Chemical Research, Kyoto University, Uji, Kyoto 611-0011, Japan. [6]Department of Chemistry, Tokyo Metropolitan University, 1-1 Minami-Osawa, Hachioji, Tokyo 192-0397, Japan. [7]RIKEN, Yokohama Institute, 1-7-22, Suehirocho, Tsurumi, Yokohama 230-0045, Japan.

space[13], DUB-mediated cleavage suggested that pyrenebutyrate/CPP_{Tat}-treatment delivered Ub-3A into the cytosol.

The concentration of transduced ^{15}N-labelled protein in the NMR sample was of the order of 20–30 μM, as estimated from the NMR signal intensities of the in-cell spectrum and the spectrum of Ub-3A recovered in the lysate (Supplementary Fig. 2b, c). The estimated concentration of endogenous ubiquitin is 13 μM, assuming that 1×10^7 cells are contained in 200 μl of the NMR sample and that each cell contains 1.5×10^8 ubiquitin molecules[14]. Leakage of ^{15}N-labelled proteins from the cells during NMR measurement was negligible, as assessed by the 1D spectrum of extracellular fluid taken from the NMR sample (Supplementary Fig. 2a). Cell viability and the integrity of the plasma membranes were assessed by staining with 0.2% (w/v) trypan blue after the completion of each NMR experiment[15]. In each case of in-cell NMR experiments shown in this paper, we found that more than 90% of cells were resistant to trypan blue uptake. This high level of cell viability and membrane integrity is consistent with the reported low toxicity of pyrenebutyrate/CPP_{Tat} treatment[8].

Having established that Ub-3A–CPP_{Tat} undergoes intracellular cleavage, we questioned whether detachment of Ub-3A from CPP_{Tat} is crucial for observing in-cell NMR spectra. We substituted the sequence G75–G76 of Ub-3A–CPP_{Tat} with two alanines to prevent intracellular cleavage by DUBs. Indeed, Ub-3A-G75A/G76A–CPP_{Tat} was resistant to cleavage in cells (Supplementary Fig. 1c). The ^1H–^{15}N correlation spectrum of cells incubated with this uncleavable protein showed a pattern typical of an aggregated protein, with several overlapping signals (Fig. 1c), indicating that liberation of ubiquitin from CPP is essential for observing well-resolved in-cell NMR spectra.

CPPs are known to show binding to acidic membrane and cytosolic components[11]. Thus, it seemed likely that the uncleaved Ub-3A-G75A/G76A–CPP_{Tat} aggregated with the inner plasma membrane or other intracellular components after delivery into the cytosol. To confirm this, we labelled the cleavable Ub-3A–CPP_{Tat} and uncleavable Ub-3A-G75A/G76A–CPP_{Tat} with the fluorescent probe Alexa-488, and observed their intracellular distribution by confocal laser-scanning microscopy. HeLa cells treated with Alexa-488-labelled Ub-3A–CPP_{Tat} showed a smooth and continuous distribution of the transduced protein throughout the cytosol and nucleus (Fig. 1d). This diffusion of internalized protein was observed in almost all cells. In contrast, treatment with the uncleavable Alexa-labelled Ub-3A-G75A/G76A–CPP_{Tat} resulted in an unsmooth and heterogeneous pattern of fluorescence in the cells, with intense staining of cytoplasmic components and nucleoli. Taken together, these results demonstrate that detachment from CPP seems to be required for both uniform distribution of the CPP-delivered proteins in the cytosol and the detection of high-resolution in-cell NMR spectra. Using Ub-3A–CPP_{Tat}, we also obtained a spectrum of Ub-3A in monkey COS-7 cells, demonstrating the universality of this method (Supplementary Fig. 3).

To measure the in-cell NMR spectra of specific proteins, we used the method of linking CPPs to cargo proteins by means of disulphide bonds[16]. In the cytosol, CPP-conjugated proteins are subject to cleavage at disulphide bonds by autonomous reduction. The ^1H–^{15}N correlation spectrum of HeLa cells treated with the B1 domain of streptococcal protein G (GB1) conjugated to CPP_{Tat} showed well-resolved signals, which could almost be superimposed on the corresponding signals in the reference *in vitro* spectrum (Fig. 2a, b). The same procedure also delivered Ub-3A into cells and gave a high-quality in-cell NMR spectrum (Fig. 2c). These results demonstrate that this method can be applied to various proteins.

The in-cell NMR experiments potentially provide a wealth of information on the conformation, dynamics and functions of proteins in the intracellular environment. The in-cell NMR spectrum of wild-type ubiquitin showed severe line-broadening effects: the intensities of most of the main-chain amide signals in the in-cell NMR spectrum (Supplementary Fig. 4) were markedly smaller than those in the spectrum of Ub-3A (Fig. 1a). In contrast, an intense signal was observed at a position corresponding to the C-terminal Gly 76 of mature ubiquitin in the in-cell spectrum of wild-type ubiquitin, as seen in Ub-3A, suggesting that the CPP was cleaved from Ub–CPP_{Tat} and that the transduced ubiquitin exists, at least partly, in a C-terminally unconjugated form in the cells. Because the mutation sites of Ub-3A (L8A, I44A and V70A) are located at the common binding interface of ubiquitin with ubiquitin-interacting proteins[17], the observation that mutation leads to a large recovery of signal intensity suggests that the line broadening observed for wild-type ubiquitin is due to its interactions with endogenous proteins. The same effect of mutation on ubiquitin was previously observed in in-cell NMR experiments using *Xenopus* oocytes[5].

In-cell NMR spectroscopy can also be applied to studying protein interactions with small compounds, such as screening drugs targeted to specific proteins. We measured the in-cell NMR spectrum of FKBP12, one of the targets of the immunosuppressants FK506 and rapamycin[18] which are often used in organ transplantation. To introduce ^{15}N-labelled FKBP12 into HeLa cells, we used another method[13] to link the protein to a cleavable CPP, by constructing a CPP_{Tat}–Ub–FKBP12 fusion protein (Fig. 3a). The fusion protein was predicted to be cleaved at the C terminus of ubiquitin by endogenous DUBs[13], thereby releasing FKBP12 into the cytosolic space. The ^1H–^{15}N correlation experiment of HeLa cells treated with ^{15}N-labelled CPP_{Tat}–Ub–FKBP12 provided an analysable high-resolution spectrum (Fig. 3a), which could be well superimposed on the reference *in vitro* spectrum (Fig. 3b), showing that the FKBP12 moiety of the fusion protein

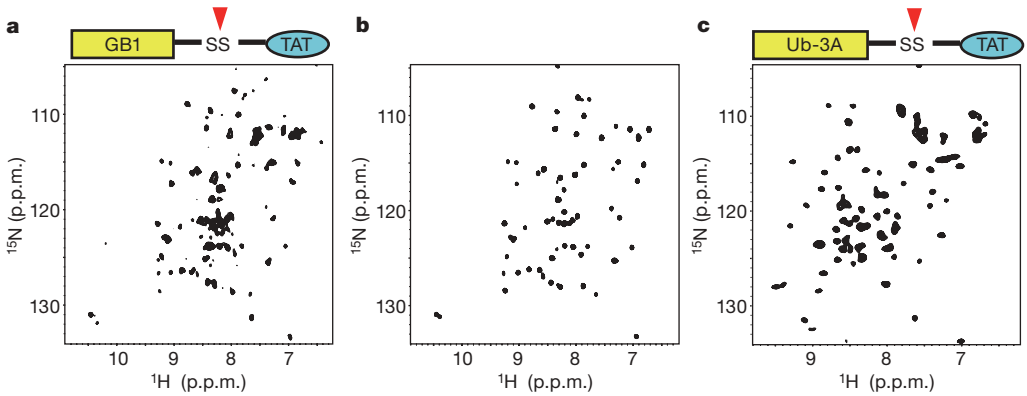

Figure 2 | In-cell spectra of proteins delivered by disulphide-linked CPP_{Tat}. **a**, In-cell ^1H–^{15}N correlation spectrum of GB1. The construct used for intracellular transduction is schematically shown above the spectrum. CPP_{Tat} is conjugated at a cysteine introduced at the C-terminal end of GB1 via a disulphide bond. The red triangle indicates the reductive cleavage site. **b**, *In vitro* reference spectrum of ^{15}N-labelled GB1. **c**, In-cell spectrum of Ub-3A transduced with CPP_{Tat} linked through a disulphide bond. The construct used is schematically shown above the spectrum. CPP_{Tat} is conjugated at a cysteine mutated at the C-terminal Gly 76 residue of Ub-3A via a disulphide bond.

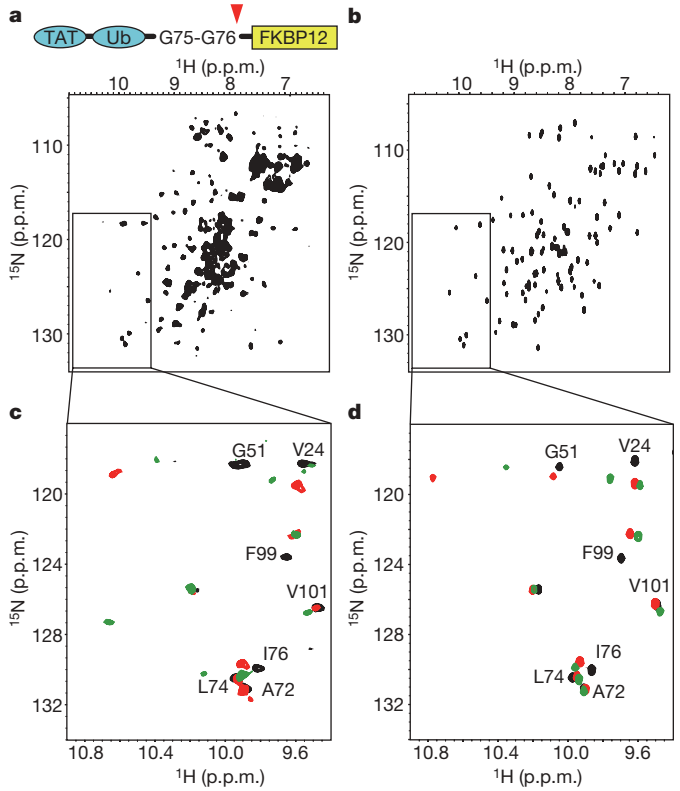

Figure 3 | In-cell NMR observation of specific complexes of FKBP12 with extracellularly administered immunosuppressants. **a**, **b**, Two-dimensional ^{1}H–^{15}N correlation spectra of HeLa cells treated with ^{15}N-labelled CPP$_{Tat}$–Ub–FKBP12 (**a**) and FKBP12 *in vitro* (**b**). The construct used is schematically shown above the spectrum in **a**. The DUB cleavage site is indicated with a red triangle. **c**, Superposition of in-cell spectra of ^{15}N-labelled FKBP12 without (black) and with administration of either FK506 (red) or rapamycin (green). **d**, Superposition of *in vitro* spectra of ^{15}N-labelled FKBP12 in the absence (black) and presence of either FK506 (red) or rapamycin (green). To generate the in-cell NMR spectra shown in **a** and **c**, data from two (spectrum in **a** and spectrum shown in red in **c**) or three (spectrum shown in green in **c**) experiments, each with a measurement time of 3 h, were added and processed.

contributed to the well-resolved cross-peaks. In contrast, the contribution from the CPP$_{Tat}$–Ub moiety seemed rather limited: a large proportion of strongly overlapping signals around the ^{1}H and ^{15}N chemical shifts of 7.8–8.5 and 119–125 p.p.m., respectively, were presumably attributable to the CPP$_{Tat}$–Ub moiety (Fig. 3a), as similar overlapping signals were observed in the in-cell spectrum of the uncleavable Ub-3A-G75A/G76A–CPP$_{Tat}$ (Fig. 1c). From these observations, we concluded that FKBP12 was released from the CPP$_{Tat}$–Ub moiety by DUB cleavage and gave analysable signals, whereas CPP$_{Tat}$–Ub aggregated with cellular components through the CPP.

We then examined the effect of externally administered immunosuppressants on the in-cell NMR spectrum of FKBP12. When the cells were incubated with FK506 after the introduction of FKBP12, several cross-peaks in the in-cell spectrum of FKBP12 were markedly different from those observed in the absence of FK506 (Fig. 3c). The in-cell NMR spectrum of FK506-treated cells showed a similar pattern to the *in vitro* reference spectrum of FKBP12 complexed with FK506 (Fig. 3d). The administration of another immunosuppressant, rapamycin, to FKBP12-containing cells gave an in-cell NMR spectrum that was distinct from the in-cell spectrum after administration of FK506, but more similar to the *in vitro* spectrum of the FKBP12–rapamycin complex (Fig. 3c, d). These results indicated that exogenously applied FK506 and rapamycin autonomously entered the cells and formed specific complexes with FKBP12. This finding demonstrates that in-cell NMR spectroscopy can act as a powerful tool for screening drugs targeting specific intracellular proteins by, first, providing information about the efficiency of drug delivery to cells, and second, establishing whether the drug makes the same interactions with the target proteins, and exerts the same structural and functional effects, as identified from *in vitro* experiments.

Proteins in cells can have dynamic properties and folding stabilities that differ from those *in vitro*, due to both specific and nonspecific interactions with intracellular macromolecules and the cytoskelton[19]. We analysed the folding stability of ubiquitin in the intracellular environment by performing a hydrogen exchange experiment coupled with in-cell NMR spectroscopy. Hydrogen exchange experiments can measure the equilibrium between folded and unfolded states of proteins, and thus reveal thermodynamic properties of proteins[20]. We transduced Ub–CPP$_{Tat}$, in which the protected amide protons were replaced by deuterons, into HeLa cells and measured the ^{1}H–^{15}N correlation spectrum of the cells to evaluate the hydrogen exchange of the main-chain amides of Val 5 and Leu 15, which are highly protected in the folded state and give well-isolated cross-peaks. We found that these amides were more highly exchanged to protons in the transduced protein than in the protein *in vitro* (Fig. 4a, b), raising the possibility that hydrogen exchange rates are increased in the intracellular environment.

To determine the exchange rates in the cells, we measured a series of spectra of ubiquitin recovered in lysates prepared by cell disruption at various times after protein transduction (Supplementary Fig. 5a). From the build-up curves of cross-peaks, the hydrogen exchange rates of all of the analysable protected amides, Val 5, Leu 15, Lys 27 and Ile 30, were approximately 15–22 times higher in cells than *in vitro* at pH 7.4 (Fig. 4c, d). Comparison of these higher exchange rates between wild-type ubiquitin and Ub-3A showed that mutation at the β-sheet surface caused a significant decrease in the amide hydrogen exchange rates (Fig. 4d and Supplementary Fig. 5b). Thus, the higher exchange rates in cells versus *in vitro* seem to be at least partly

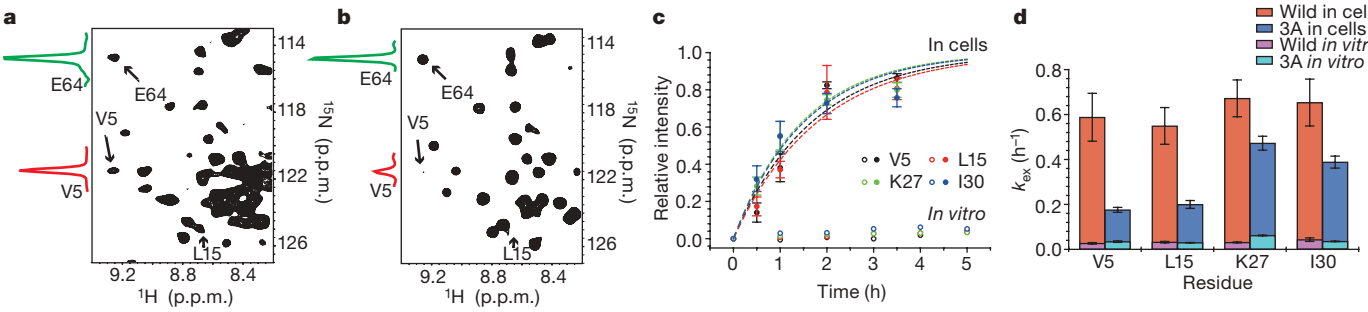

Figure 4 | Hydrogen exchange experiments. **a**, ^{1}H–^{15}N correlation spectrum of HeLa cells treated with ^{15}N-labelled deuterated Ub–CPP$_{Tat}$. Data from two experiments, each with a measurement time of 3 h, were added. **b**, *In vitro* reference spectrum of ^{15}N-labelled deuterated Ub–CPP$_{Tat}$. Slices at ^{1}H frequencies of Val 5 (red) and Glu 64 (green) are also shown. The amide of Glu 64 is unprotected even in the folded state. **c**, Build-up of cross-peaks of protected amides in the spectra of ubiquitin recovered in lysates collected at various times after protein transductions (filled symbols). Those *in vitro* at pH 7.4 are also shown (open symbols). For the lysates, averaged values over three independent trials are plotted with standard deviations. **d**, The hydrogen exchange rates (k_{ex}) in cells and *in vitro* at pH 7.4 of protected amides in ubiquitin and Ub-3A. Bars indicate standard errors.

due to interactions of ubiquitin with endogenous interacting proteins, as the mutation sites of Ub-3A are located at the common binding interface of ubiquitin with them[17]. Ubiquitin exhibits large structural heterogeneity both in itself and after binding to different partners[21]. Thus, binding to various proteins in cells might cause interconversion between different conformations of ubiquitin, which may destabilize folding and increase hydrogen exchanges rates. Alternatively, some of these proteins may preferentially bind to less folded states of ubiquitin. The observation that Ub-3A still showed significantly higher exchange rates in cells than *in vitro* raises the possibility that nonspecific interactions with other macromolecules, the cytoskeleton and inner membranes may also decrease the folding stability of ubiquitin in cells (Fig. 4d). This result may challenge the general belief that the folding of proteins inside cells is stabilized through macromolecular crowding and macromolecular confinement effects[19]. A comprehensive analysis will be required to determine the mechanism and generality of the observed intracellular increase in hydrogen exchange rate by examining various proteins and cell types in the future.

In this report, we show that high-resolution in-cell NMR spectroscopy of proteins enables the investigation of the structures, functions and folding stabilities of specific proteins using human cells in an intracellular environment. Our results demonstrate that detachment of the proteins from CPPs yields a homogeneous dispersion of labelled proteins in the cytosol, which allows the proteins to form specific protein–protein and protein–drug complexes. Protein transduction by CPPs have been shown to be applicable to a variety of cells, including established cell strains, primary cultured cells and even cells of living animals[10–12,22]. Thereby, the present in-cell NMR technique opens up a multitude of different applications, such as the study of protein dynamics, investigations of amyloid-forming or intrinsically unstructured proteins in neuronal cells, and molecular diagnostics by observing probe proteins in biopsy specimens.

METHODS SUMMARY

Protein transduction to HeLa cells for in-cell NMR spectroscopy. Protein transduction into HeLa cells was carried out as described previously[8] with modifications. Approximately 2×10^6 cells were plated into two 90-mm Petri dishes and incubated in DMEM medium containing 10% FBS (Thermo Fisher Scientific), penicillin and streptomycin for 48 h under 5% CO_2 humidified atmosphere. After removing the medium, the cells were washed twice with PBS. The cells were incubated with 1-pyrenebutyric acid (Sigma-Aldrich) in PBS for 5 min at 37 °C, and then the CPP-linked protein dissolved in PBS was added. The final concentrations of both pyrenebutyrate and protein were 250 μM. After a 10-min incubation at 37 °C, the cells were washed five times with PBS. The pyrenebutyrate/CPP-treatment was repeated four times. After each of the four rounds of treatment, the cells were incubated for 40 min at 37 °C in medium. The cells were then detached from the dish by treatment with 0.01% (w/v) trypsin (5 ml per dish) for 10 min at 37 °C. The cells were then gently suspended in 20 ml of the medium containing 5 mM HEPES (pH 7.2) and 90 mM D-glucose. The resulting cell suspension (30 ml) was incubated for 30 min at 37 °C, and then centrifuged at 100*g* for 5 min at room temperature. Finally, the cell pellet was resuspended in DMEM containing 5 mM HEPES (pH 7.2), 90 mM D-glucose and 5% D_2O, yielding 200 μl of cell suspension, which was used for the NMR measurements.

NMR spectroscopy. In-cell and the reference 2D ^1H–^{15}N correlation NMR spectra were obtained using the band-selective optimized flip-angle short transient (SOFAST)-heteronuclear multiple quantum coherence (HMQC) pulse sequence[23]. The data for the indirectly acquired dimension (^{15}N) were acquired by a nonlinear sampling scheme and processed by maximum-entropy reconstruction[24], except for those of cell lysates.

Full Methods and any associated references are available in the online version of the paper at www.nature.com/nature.

Received 16 October 2008; accepted 23 January 2009.

1. Serber, Z. & Dotsch, V. In-cell NMR spectroscopy. *Biochemistry* **40,** 14317–14323 (2001).
2. Burz, D. S., Dutta, K., Cowburn, D. & Shekhtman, A. Mapping structural interactions using in-cell NMR spectroscopy (STINT-NMR). *Nature Methods* **3,** 91–93 (2006).
3. Dedmon, M. M., Patel, C. N., Young, G. B. & Pielak, G. J. FlgM gains structure in living cells. *Proc. Natl Acad. Sci. USA* **99,** 12681–12684 (2002).
4. Sakakibara, D. *et al.* Protein structure determination in living cells by in-cell NMR spectroscopy. *Nature* doi:10.1038/nature07814 (this issue).
5. Sakai, T. *et al.* In-cell NMR spectroscopy of proteins inside *Xenopus laevis* oocytes. *J. Biomol. NMR* **36,** 179–188 (2006).
6. Selenko, P. *et al.* Quantitative NMR analysis of the protein G B1 domain in *Xenopus laevis* egg extracts and intact oocytes. *Proc. Natl Acad. Sci. USA* **103,** 11904–11909 (2006).
7. Selenko, P. *et al.* In situ observation of protein phosphorylation by high-resolution NMR spectroscopy. *Nature Struct. Mol. Biol.* **15,** 321–329 (2008).
8. Takeuchi, T. *et al.* Direct and rapid cytosolic delivery using cell-penetrating peptides mediated by pyrenebutyrate. *ACS Chem. Biol.* **1,** 299–303 (2006).
9. Futaki, S. Oligoarginine vectors for intracellular delivery: design and cellular-uptake mechanisms. *Biopolymers* **84,** 241–249 (2006).
10. Nakase, I., Takeuchi, T., Tanaka, G. & Futaki, S. Methodological and cellular aspects that govern the internalization mechanisms of arginine-rich cell-penetrating peptides. *Adv. Drug Deliv. Rev.* **60,** 598–607 (2008).
11. Wender, P. A. *et al.* The design of guanidinium-rich transporters and their internalization mechanisms. *Adv. Drug Deliv. Rev.* **60,** 452–472 (2008).
12. Schwarze, S. R., Ho, A., Vocero-Akbani, A. & Dowdy, S. F. *In vivo* protein transduction: delivery of a biologically active protein into the mouse. *Science* **285,** 1569–1572 (1999).
13. Loison, F. *et al.* A ubiquitin-based assay for the cytosolic uptake of protein transduction domains. *Mol. Ther.* **11,** 205–214 (2005).
14. Carlson, N. & Rechsteiner, M. Microinjection of ubiquitin - intracellular-distribution and metabolism in Hela-cells maintained under normal physiological conditions. *J. Cell Biol.* **104,** 537–546 (1987).
15. O'Brien, R. & Gottlieb-Rosenkrantz, P. An automatic method for viability assay of cultured cells. *J. Histochem. Cytochem.* **18,** 581–589 (1970).
16. Giriat, I. & Muir, T. W. Protein semi-synthesis in living cells. *J. Am. Chem. Soc.* **125,** 7180–7181 (2003).
17. Hicke, L., Schubert, H. L. & Hill, C. P. Ubiquitin-binding domains. *Nature Rev. Mol. Cell Biol.* **6,** 610–621 (2005).
18. Itoh, S. & Navia, M. A. Structure comparison of native and mutant human recombinant FKBP12 complexes with the immunosuppressant drug FK506 (tacrolimus). *Protein Sci.* **4,** 2261–2268 (1995).
19. Ellis, R. J. Macromolecular crowding: obvious but underappreciated. *Trends Biochem. Sci.* **26,** 597–604 (2001).
20. Bai, Y. *et al.* Thermodynamic parameters from hydrogen exchange measurements. *Methods Enzymol.* **259,** 344–356 (1995).
21. Lange, O. F. *et al.* Recognition dynamics up to microseconds revealed from an RDC-derived ubiquitin ensemble in solution. *Science* **320,** 1471–1475 (2008).
22. Delom, F., Fessart, D., Caruso, M. E. & Chevet, E. Tat-mediated protein delivery in living *Caenorhabditis elegans*. *Biochem. Biophys. Res. Commun.* **352,** 587–591 (2007).
23. Schanda, P. & Brutscher, B. Very fast two-dimensional NMR spectroscopy for real-time investigation of dynamic events in proteins on the time scale of seconds. *J. Am. Chem. Soc.* **127,** 8014–8015 (2005).
24. Laue, E. D., Mayger, M. R., Skilling, J. & Staunton, J. Reconstruction of phase-sensitive two-dimensional NMR-spectra by maximum-entropy. *J. Magn. Reson.* **68,** 14–29 (1986).

Supplementary Information is linked to the online version of the paper at www.nature.com/nature.

Acknowledgements We thank M. Waelchli, A. Kidera and H. Akutsu for discussion, T. Kokubo for monkey COS-7 cells, H. Ohnishi for the plasmid for production of FKBP12 and M. Imanishi for taking gel fluorimaging. This work was supported by grants to M.S. from Japan Science and Technology Agency and the Ministry of Education, Culture, Sports, Science and Technology-Japan (MEXT), and also in part by the Global COE Program 'International Center for Integrated Research and Advanced Education in Materials Science' (No. B-09) of MEXT, administered by the Japan Society for the Promotion of Science. This work was partly supported by the Innovative Techno-Hub for Integrated Medical Bio-imaging Project of the Special Coordination Funds for Promoting Science and Technology, from MEXT to A.O. and M.S., and by grants from MEXT to S.F. and H.T.

Author Information Reprints and permissions information is available at www.nature.com/reprints. Correspondence and requests for materials should be addressed to M.S. (shirakawa@moleng.kyoto-u.ac.jp) or H.T. (tochio@moleng.kyoto-u.ac.jp).

METHODS

Protein preparation. All proteins used to obtain the in-cell and reference NMR spectra were expressed in *E. coli* BL21(DE3), grown in M9 minimal medium containing $^{15}NH_4Cl$ as the sole nitrogen source. Ub–CPP_{Tat} and its derivatives, which contain an extra aspartic acid at the amino terminus of CPP_{Tat}, were purified as described previously[25]. A GB1 fusion protein that has a thrombin cleavable N-terminal 6-His-tag and a cysteine residue at its N and C terminuses, respectively, was purified using a similar procedure. After the His-tag was removed, GB1-SS–CPP_{Tat} was prepared using the GB1 derivative and Cys-(NPyS, 3-nitro-2-pyridinesulfenyl)–CPP_{Tat}[26] (TORAY RESEARCH CENTER Inc.) as described[16]. To generate Ub-3A-SS–CPP_{Tat} (Fig. 2c), Ub-3A with a cysteine substitution at Gly 76 was used. The GST–SUMO1–CPP_{Tat}–Ub–FKBP12 fusion protein, which has an additional DGA sequence between ubiquitin and FKBP12, was expressed, and was purified by glutathione (GSH) affinity chromatography. After cleavage by the catalytic domain of SENP2, the CPP_{Tat}–Ub–FKBP12 fusion protein was purified by chromatography.

Immunosuppressant administration. HeLa cells were treated with ^{15}N-labelled CPP_{Tat}–Ub–FKBP12 as described above, and were detached from the dishes, collected by gentle centrifugation and suspended in 20 ml of a medium/buffer cocktail containing 30 μM FK506 or rapamycin. The cell suspension was incubated for 1 h at 37 °C, and then centrifuged at 100*g* for 5 min. Finally, the cell pellet was resuspended in DMEM containing 5 mM HEPES (pH 7.2), 90 mM D-glucose, 5% D_2O, and 30 μM FK506 or rapamycin, yielding 200 μl of cell suspension, which was used for the NMR measurements. The resonance assignments of unliganded FKBP12 are on the basis of a previous report[27].

NMR experiments. All NMR experiments were performed at 37 °C on a Bruker Avance 700 spectrometer equipped with a cryogenic TCI probe head. The volume of each cell suspension used for NMR measurements was approximately 200 μl. NMR sample tubes with a diameter of 4 mm (Shigemi) were used for in-cell NMR measurements. All the 2D ^1H–^{15}N correlation spectra were acquired using a SOFAST-HMQC pulse sequence[23]. The spectral widths were 5597.015 Hz and 2128.792 Hz for ^1H and ^{15}N, respectively. Data in the indirectly acquired ^{15}N dimension were sampled non-uniformly and processed by the maximum-entropy procedure[24], unless mentioned otherwise. Thirty-two time-points were randomly selected from 64 conventional linear sampling points with a t_{1max} of 7.52 ms. The final size of the matrix reconstructed was 512 (F_2) × 256 (F_1) complex points. Measurement of each in-cell NMR sample took no longer than 3 h. Data were processed by NMRPipe[28] or AZARA 2.7 software (http://www.bio.cam.ac.uk/azara/), and analysed with Sparky[29].

Assessment of cell viability after in-cell NMR experiments. The viability of the cells after each in-cell NMR experiment was checked by trypan blue staining[15]. The cells recovered from the NMR tube were mixed with 0.2% (w/v) trypan blue, and the number of stained cells was counted under phase-contrast microscope.

Hydrogen exchange experiments. Replacement of the exchangeable protons of Ub–CPP_{Tat} with ^2H was achieved by unfolding the protein using 6 M guanidium hydrochloride in PBS (pH 7.3) containing D_2O. The protein was then refolded by repeated dialysis against PBS in D_2O. Finally, the sample was dialysed against PBS (pH 7.3) in H_2O. At this stage, only highly protected amides were deuterated. The deuterated protein was transduced into HeLa cells as described in the Methods Summary, except for the incubation temperature, which was room temperature. Data for the ^1H–^{15}N-correlation spectrum of the cells were then collected at 37 °C for 3 h. For an *in vitro* reference, deuterated Ub–CPP_{Tat} was incubated in PBS (pH 7.3) at room temperature for 6 h and at 37 °C for 5 h, and then the spectrum was measured for 5 min. To measure hydrogen exchange rates in cells, Ub–CPP_{Tat} and Ub-3A–CPP_{Tat}, in which the protected amides were deuterated, were transduced into HeLa cells as described above, except for times of pyrenebutyrate/CPP treatment, which were two. In addition, the treatments were done without an interval incubation. This procedure of pyrenebutyrate/CPP treatment took 30 min in total. The cells were then incubated at 37 °C until they were collected for disruption, except for the experiments for data collected at a time point of 30 min, in which the cells were collected for disruption immediately after the pyrenbutyrate/CPP treatment. At 30, 60, 120 and 210 min after the start of protein transduction, the cells were detached from the dishes, washed and disrupted in 100 mM ammonium acetate and 50 mM sodium chloride (pH 5) to obtain cell lysates. The lysates were concentrated approximately 1.5-fold by Microcon-YM3 (Millipore). ^1H–^{15}N SOFAST-HMQC spectra of the lysates were acquired at 37 °C for 20 h by a linear sampling scheme and processed by Fourier transformation. Three independent experiments were performed for each time point. The signal intensities of the main-chain amides of Val 5, Leu 15, Lys 27 and Ile 30 were used for the analysis, because they were invariant for at least 20 h *in vitro* at pH 5. The cross-peak intensities were normalized by the averaged intensities of the main-chain amides of 14 residues, the hydrogens of which rapidly exchange with water even in the folded state.

To estimate the variance of the cross-peak intensities due to intracellular effects other than hydrogen exchange, we performed the same procedure using fully protonated proteins. The signal intensities were used to normalize the hydrogen exchange data. Furthermore, the protonation ratios of the samples used for the protein transductions were assessed by *in vitro* spectra, and were used to correct intensity data. The normalized intensities at time t after the start of protein transduction, Int (t), were fitted to the equation $\mathrm{Int}(t) = 1 - \exp(-k_{ex}t)$, in which k_{ex} is the hydrogen exchange rate. To obtain k_{ex} values for the *in vitro* condition, ^1H–^{15}N SOFAST-HMQC spectra were acquired for ubiquitin every 24 h for 3 days in PBS (pH 7.4) at 37 °C, and for Ub-3A every 2 h for 12 h. One experiment was performed for each time point.

Confocal laser-scanning microscopy. To generate Alexa-labelled Ub-3A–CPP_{Tat} and Ub-3A-G75A/G76A–CPP_{Tat}, proteins with a cysteine substitution of Gly 35 were treated with Alexa-Fluor-488 C5 maleimide (Invitrogen). Unliganded fluorescent reagent was removed using a PD-10 column (GE Healthcare). The ratios between the labelled and unlabelled proteins were approximately 0.1. Next, 2×10^5 HeLa cells were plated into 35-mm glass-bottomed dishes and cultured for 48 h. The cells were treated first with 50 μM pyrenebutyrate for 5 min, and then with 75 μM protein in the presence of 50 μM pyrenebutyrate for 10 min. Distribution of the Alexa-labelled proteins in HeLa cells was analysed without fixing using a confocal laser-scanning microscope (Olympus FV300) equipped with a ×60 objective lens. The fluorescence signals were detected by excitation with the 488-nm Argon laser using an emission filter (510–530 nm).

25. Tenno, T. *et al.* Structural basis for distinct roles of Lys63- and Lys48-linked polyubiquitin chains. *Genes Cells* **9**, 865–875 (2004).
26. Mezo, G., Mihala, N., Andreu, D. & Hudecz, F. Conjugation of epitope peptides with SH group to branched chain polymeric polypeptides via Cys(Npys). *Bioconjug. Chem.* **11**, 484–491 (2000).
27. Rosen, M. K., Michnick, S. W., Karplus, M. & Schreiber, S. L. Proton and nitrogen sequential assignments and secondary structure determination of the human FK506 and rapamycin binding protein. *Biochemistry* **30**, 4774–4789 (1991).
28. Delaglio, F. *et al.* NMRPipe: a multidimensional spectral processing system based on UNIX pipes. *J. Biomol. NMR* **6**, 277–293 (1995).
29. Goddard, T. D. & Kneller, D. G. SPARKY 3 (University of California, 1999).